

Low-energy Electron Scattering from Polyatomic Molecules: The Role of Electron Correlation*

C. William McCurdy

Lawrence Livermore National Laboratory,
National Energy Research Supercomputer Center, L-561,
7000 East Ave, P.O. Box 5509, Livermore, CA 94550, U.S.A.

Abstract

Until recently the principal barrier to the accurate theoretical description of electronic collisions with polyatomic molecules was the problem of scattering by a nonlocal potential which is arbitrarily asymmetric. The last five or six years have seen the development of numerical techniques capable of solving the potential scattering problem, and the first applications of methods for treating many-body aspects of collisions of electrons with polyatomic molecules are beginning to appear in the literature. We describe the complex Kohn method and the use, in scattering calculations, of methods for treating electronic correlation which are standard in bound-state quantum chemistry. As examples of the application of these ideas we present the results of calculations on electron scattering from CH_4 , SiH_4 and C_2H_6 . All of these molecules exhibit Ramsauer–Townsend minima at low impact energies which are entirely correlation effects.

1. Introduction

Theoretical treatments of electron–molecule collisions are complicated by an obvious problem, which it is useful to revisit occasionally. The problem is most easily exposed by examining the close-coupling expansion (Taylor 1972), but it is inherent in the electronic collision problem and not a consequence of a particular representation of the scattering wavefunction. The close-coupling expansion of a scattering wavefunction Ψ , in terms of target states in the case that the projectile and target particles are distinguishable, is simply

$$\Psi = \sum_{\Gamma} \chi_{\Gamma}(x) F_{\Gamma}(\mathbf{r}), \quad (1)$$

where $\chi_{\Gamma}(x)$ is a state of the target, which may be an energetically open or closed channel, and $F_{\Gamma}(\mathbf{r})$ is the channel wavefunction for relative motion of the projectile and target. If only a single channel is included in the expansion, then inserting (1) in the Schrödinger equation leads to the problem of finding the solution, $F_{\Gamma}(\mathbf{r})$, for scattering from a local potential. That situation would obtain in electron scattering *except* for the fact that electrons are indistinguishable particles and the scattering wavefunction must be antisymmetric with respect to

* Paper presented at the Joint Symposium on Electron and Ion Swarms and Low Energy Electron Scattering, held at Bond University, Queensland, 18–20 July 1991.

the interchange of their coordinates. For electronic collisions (1) is replaced by

$$\Psi = \sum_{\Gamma} \mathbf{A} \{ \chi_{\Gamma}(\mathbf{r}_1, \dots, \mathbf{r}_n) F_{\Gamma}(\mathbf{r}_{n+1}) \}, \quad (2)$$

where \mathbf{A} is the antisymmetriser and \mathbf{r}_j is the coordinate of the j th electron. The insertion of (2) in the Schrödinger equation leads to the problem of scattering from *nonlocal* potentials because of the antisymmetriser. That difficulty is only one of the consequences of the fact that the incident electron is indistinguishable from those in the target. A more subtle, and ultimately more important, consequence is that the electron correlation between the incident electron and those of the target, which is displayed in the expansion in (2), is *inextricably connected* to correlation among the electrons of the target. Consistency in the treatment of both aspects of electronic correlation in the electron-molecule scattering problem is essential, even though it is not always obvious how to formulate a consistent treatment.

In the theoretical description of electronic collisions with molecules a great deal of effort has been expended in the development of methods for the treatment of the basic problem of scattering from an asymmetric, nonlocal potential (Lane 1980; Takasuka and McKay 1981, 1984; McCurdy and Rescigno 1989). To attack the problem of arbitrary polyatomic targets, approaches are needed which avoid single centre expansions, and which are highly efficient. In recent years several methods have appeared, including the one on which we focus here, the complex Kohn method.

Since the problem of electron correlation connects the scattering and bound-state portions of the theoretical description of electronic collisions, it is important for any method to be able to treat all electron correlation on the same footing. For that reason it is highly desirable to be able to formulate the scattering problem in such a way that the arsenal of computational tools developed for quantum chemistry is easily incorporated into the scattering calculation.

The complex Kohn method (Miller and Jansen op de Haar 1987; McCurdy *et al.* 1987; Rescigno *et al.* 1989, 1990; McCurdy and Rescigno 1989; Parker *et al.* 1991) is based on a variational principle for the T -matrix, T^{Γ, Γ_0} , for transitions between states Γ and Γ_0 , which takes the form

$$T^{\Gamma, \Gamma_0}[\Psi_{\Gamma}, \Psi_{\Gamma_0}] = T_{\text{trial}}^{\Gamma, \Gamma_0} - 2 \int \Psi_{\Gamma} (H - E) \Psi_{\Gamma_0}, \quad (3)$$

where $T_{\text{trial}}^{\Gamma, \Gamma_0}$ appears in the asymptotic forms of the trial wavefunctions Ψ_{Γ} and Ψ_{Γ_0} as described in the following section. The advantages of this approach arise largely because the working equations which devolve from (3) involve only matrix elements of the Hamiltonian H , and therefore the connection with and incorporation of techniques of bound-state quantum chemistry is as straightforward as possible.

In the following section we outline the complex Kohn method and describe the correlated trial wavefunction which is employed in the elastic scattering calculations we present here. In Section 3 we describe some results for electronic collisions with methane, silane and ethane. Finally, in Section 4, we discuss how

the problem of consistency between the treatment of correlation in the target and in the $(N + 1)$ -electron scattering system is addressed by the simple *ab initio* approach we illustrate here.

2. Theory

(2a) Complex Kohn Method for Electron–Molecule Scattering

The complex Kohn method has been discussed at length in a number of papers, and has recently been employed in several studies of low-energy electron–molecule scattering (Miller and Jansen op de Haar 1987; McCurdy *et al.* 1987; Rescigno *et al.* 1989, 1990; McCurdy and Rescigno 1989; Parker *et al.* 1991; Lengsfeld *et al.* 1991). For that reason we only briefly outline the method here and discuss the form of the trial scattering function that is employed in the Kohn calculations reported below.

For application to electron scattering we tailor the trial wavefunction to make the interface with electronic structure calculations easy. The sum in (2) is partitioned to separate the contributions of open and closed channels. Furthermore the closed channel contributions, which can be thought of as $(N + 1)$ -electron correlation terms, are expressed in terms of $(N + 1)$ -electron configurations of Gaussian orbitals. Thus the trial scattering wavefunction for scattering from an initial state Γ' is chosen to be of the form

$$\Psi_{\Gamma'} = \sum_{\Gamma} A\{\chi_{\Gamma}(\mathbf{r}_1, \dots, \mathbf{r}_n) F_{\Gamma\Gamma'}(\mathbf{r}_{n+1})\} + \sum_{\mu} d_{\mu}^{\Gamma'} \Xi_{\mu}(\mathbf{r}_1, \dots, \mathbf{r}_{n+1}). \quad (4)$$

The one-electron scattering orbitals $F_{\Gamma\Gamma'}$ are expanded in Bessel functions and cartesian Gaussians as explained in McCurdy and Rescigno (1989):

$$F_{\Gamma\Gamma'} = \sum_{\sigma} c_{\sigma}^{\Gamma\Gamma'} \varphi_{\sigma} + \sum_{lm} (f_{lm}^{\Gamma} \delta_{mm'} \delta_{ll'} \delta_{\Gamma\Gamma'} + T_{lm'l'm'}^{\Gamma\Gamma'} g_{lm}^{\Gamma}), \quad (5)$$

where f_{lm}^{Γ} and g_{lm}^{Γ} are incoming and outgoing continuum functions respectively. The continuum functions behave asymptotically as linearly independent regular and outgoing Ricatti–Bessel and Hankel functions,

$$f_{lm}^{\Gamma} \sim k_{\Gamma}^{-1/2} \sin(k_{\Gamma} r - l\pi/2) \quad \text{as } r \sim \infty, \quad (6)$$

$$g_{lm}^{\Gamma} \sim k_{\Gamma}^{-1/2} \exp[i(k_{\Gamma} r - l\pi/2)] \quad \text{as } r \sim \infty. \quad (7)$$

The square-integrable scattering functions φ_{σ} in (5) are orthogonal to the orbitals occupied in the target wavefunctions, χ_{Γ} . The $(N + 1)$ -electron configuration state functions (CSFs) Ξ_{μ} which appear in (5) are used, as noted above, to incorporate the effects of closed channels [and therefore $(N + 1)$ -electron correlation] in the trial scattering function. In cases where there are open shell contributions to the target wavefunction, some of these $(N + 1)$ -electron CSFs are needed to relax the constraint that the one-electron scattering function $F_{\Gamma\Gamma'}$ be orthogonal to the orbitals occupied in the target wavefunction.

The calculations we report here are for elastic scattering so there is only one state χ_{Γ} , and the closed channels are included in the second term in (4). In

this study, we employ a trial scattering function we call a polarised-SCF trial scattering function. In this case χ_Γ is a self-consistent field (SCF) wavefunction for the ground state, and the closed channels are single excitations from the SCF wavefunction as described below. The T matrix elements, $T_{lml'm'}^{\Gamma\Gamma'}$, appearing in (5) are the fundamental dynamical quantities which determine the scattering cross sections. The stationary expression for the T matrix is obtained by differentiating the Kohn functional

$$T[\Psi] = T_{\text{trial}} - 2 \int (P\Psi)(H_{\text{eff}} - E)(P\Psi), \quad (8)$$

where the Feshbach projection operator P projects on the open-channel space. In (8) Feshbach partitioning has been used to define an effective Hamiltonian

$$H_{\text{eff}} = H_{PP} + H_{PQ}(E - H_{QQ})^{-1}H_{QP} \quad (9)$$

$$= H_{PP} + V_{\text{opt}}. \quad (10)$$

The energy-dependent optical potential V_{opt} describes target polarisation and relaxes the orthogonality constraints imposed on the one-electron scattering function $F_{\Gamma\Gamma'}$. In equations (8)–(10) the P -space consists of all the configurations generated by the first term in (4), which is denoted as $(P\Psi)$ in (8), and the Q -space is composed of the $(N + 1)$ -electron configurations Ξ_μ in the second term of this equation. The $(N + 1)$ -electron configuration state functions (CSFs) comprising Q -space in this trial function have been formally incorporated into the optical potential and will not explicitly appear in the T -matrix expression in this formulation of the Kohn method. Polarisation is introduced in this trial function by including in Q -space those $(N + 1)$ -electron CSFs that are the direct product of closed-channel wavefunctions and square-integrable functions. In the polarised-SCF trial function employed in this study, closed-channel wavefunctions are generated by singly exciting the orbitals occupied in the SCF wavefunction of the target. Instead of using all of the virtual orbitals to define a space of singly excited CSFs, only a subset of these virtual orbitals, the polarised virtual orbitals, is used (Lengsfeld *et al.* 1991). The polarisability obtained from the closed channels described in this reduced singly excited space is found to agree with the value obtained in the calculations which employed the full singly excited virtual orbital space to one per cent. This transformation to the polarised orbital basis produces a much more compact trial function and also provides a better balance of the short-range interactions which arise in these calculations. This last point was discussed in some detail in Lengsfeld *et al.* (1991). The transformation that is used to define this polarised virtual orbital subspace will be discussed in the next section.

Finally, we note that the entire discussion in this section has treated the coordinates of the nuclei of the molecule as fixed parameters. Thus, these calculations are done in the ‘fixed-nuclei’ approximation, and the T -matrix in (3) and (5) provides the information necessary to construct total and differential scattering cross sections within the framework of that approximation. The procedure for doing so is discussed in McCurdy and Rescigno (1989) and Rescigno

et al. (1990), and requires an average of the cross section over molecular orientations. Dynamical coupling of the electronic motion to the rotational and vibrational degrees of freedom is neglected in fixed-nuclei calculations, although one may approximate the effects of these couplings using theories which exploit the parametric dependence of the T -matrix on the nuclear coordinates (Lane 1980).

(2b) Polarised Orbitals

The notion of a polarised orbital in scattering calculations can be said to have originated with the polarised orbital method of Callaway (1957), Callaway *et al.* (1968), Temkin and Lamkin (1961). We have discussed its adaptation and refinement in the context of the complex Kohn method elsewhere (Lengsfeld *et al.* 1991), but we summarise it here because it is essential to the physics of the polarised-SCF trial function.

The first order perturbation theory expression for a component of the dipole polarisability of an atom or molecule is

$$\alpha_k = 2 \sum_{i \neq 0} \frac{\langle \Psi_i | \mu_k | \Psi_0 \rangle^2}{E_i - E_0}, \quad (11)$$

where μ_k is a component of the dipole operator, Ψ_0 is the target wavefunction and E_0 is its energy. Here Ψ_i is an excited state wavefunction with energy E_i . If we adopt an independent orbital approximation, where one orbital will be polarised and all of the other orbitals frozen, this polarisability expression reduces to a simpler form which only requires the construction of one-electron Fock operators,

$$\alpha_{n,k} = 2 \sum_{i \neq n}^{\text{virtual}} \frac{\langle \varphi_i | \mu_k | \varphi_n \rangle^2}{\epsilon_i - \epsilon_n}, \quad (12)$$

where φ_n is the Hartree-Fock (HF) orbital that is being polarised and ϵ_n is its HF eigenvalue. In order to employ this simple polarisability expression the virtual orbitals must be eigenfunctions of a one-electron V_{N-1} Fock operator, and thus in (12) φ_i is an improved virtual orbital (IVO), an eigenvector of the one-electron IVO or V_{N-1} Hamiltonian, F_{IVO} , with eigenvalue ϵ_i :

$$F_{\text{IVO}} = T_e + V_{\text{nuc}} + 2J_m - K_m + J_n + K_n. \quad (13)$$

Here T_e is a one-electron kinetic energy operator, V_{nuc} is the electron-nuclear attraction operator, and J_m and K_m are the Coulomb and exchange operators for the set of doubly occupied orbitals, less the orbital that is being polarised. Further, J_n and K_n are the Coulomb and exchange operators of the valence orbital that is being polarised. Similarly, in this independent-orbital approximation the expression for a first-order perturbed orbital is

$$\varphi_{n,k}^1 = \sum_i^{\text{virtual}} \frac{\varphi_i \langle \varphi_i | \mu_k | \varphi_n \rangle}{\epsilon_i - \epsilon_n}. \quad (14)$$

It can be easily seen that this orbital can also be constructed by diagonalising the matrix (Lengsfeld *et al.* 1991)

$$\rho_{ij}^{n,k} = \frac{\langle \varphi_i | \mu_k | \varphi_n \rangle \langle \varphi_n | \mu_k | \varphi_j \rangle}{(\epsilon_i - \epsilon_n)(\epsilon_j - \epsilon_n)} \quad (15)$$

This operator has the property that it has at most one nonzero, positive eigenvalue. The eigenvectors of this operator are the polarised virtual orbitals we seek. In general, three polarised orbitals will be generated for each occupied valence orbital, one orbital being generated for each component of the dipole operator. Fewer than three polarised orbitals will be obtained if the Gaussian basis set does not contain $(l + 1)$ angular momentum functions, where l is the angular momentum of the orbital being polarised. This procedure is repeated for each occupied orbital shell and the resulting polarised orbitals are orthogonalised. The closed-channel wavefunctions that are used to define Q -space in our Kohn calculations are then constructed by singly exciting the valence orbitals into the polarised orbital space.

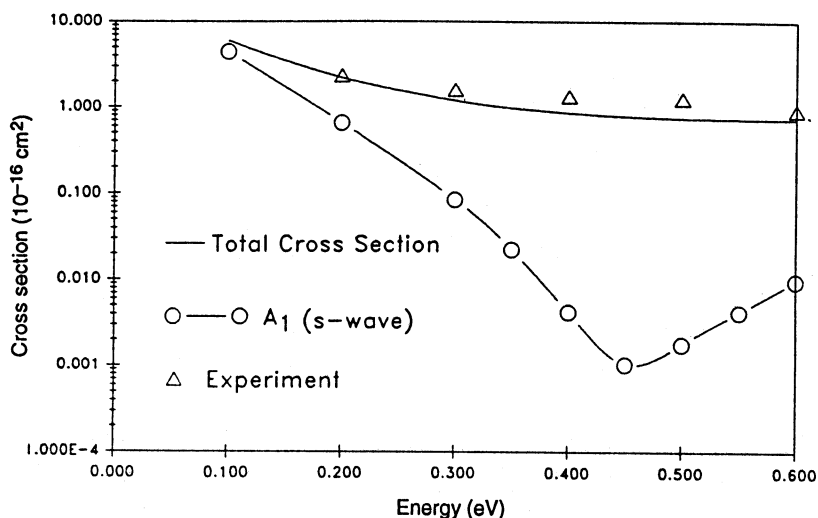


Fig. 1. Low-energy cross sections obtained for elastic electron-methane collisions. Experimental results are from Sohn *et al.* (1986).

3. Results of Calculations on Electronic Collisions with Polyatomic Targets

(3a) Low-energy Electron-CH₄ Collisions

Our calculations for methane make use of a contracted Gaussian basis consisting of (12s, 6p)/[8s, 4p] on the carbon, (6s, 1p)/[3s, 1p] on the hydrogens, and an additional diffuse s-type function on the hydrogens together with (1s, 2p, 5d) diffuse functions on the carbon. It is well known that the static-exchange approximation fails to produce any Ramsauer-Townsend (RT) minimum in the cross section for this molecule (Lengsfeld *et al.* 1991; Lima *et al.* 1989). In Fig. 1 we compare our polarised SCF results with experimental values below

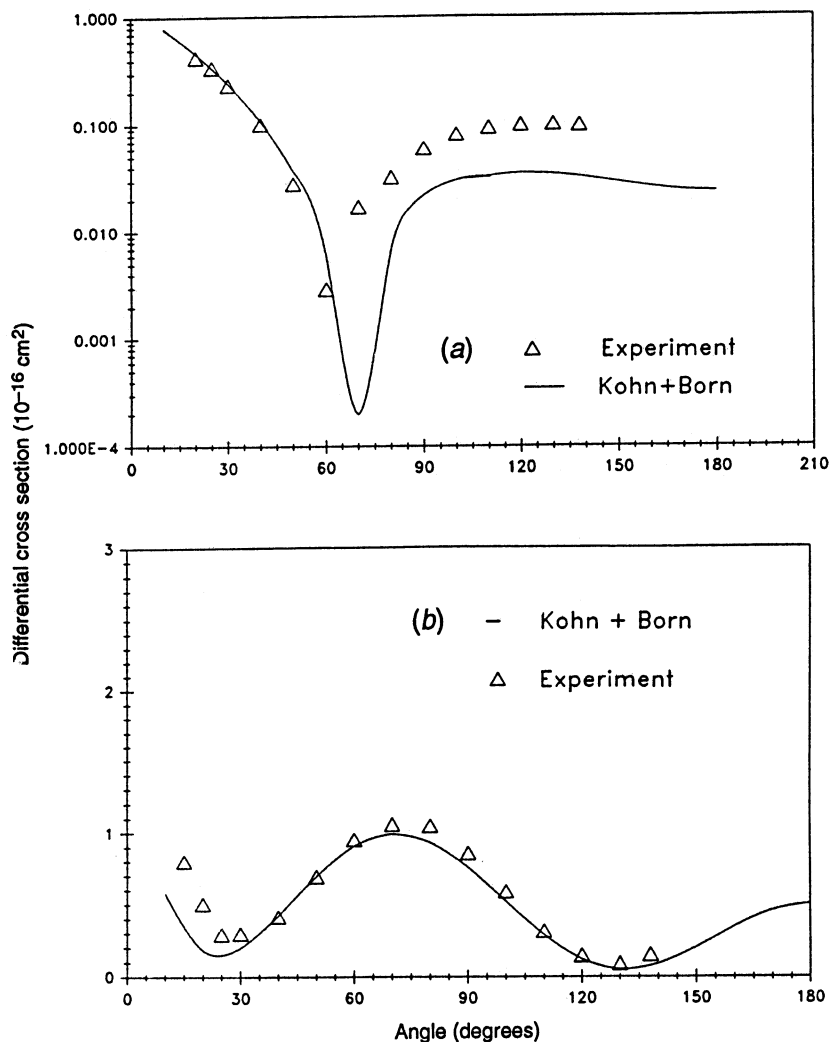


Fig. 2. Differential cross sections at (a) 0.5 eV and (b) 3.0 eV with $l < 2$ contributions from the polarised-Born approximation. Triangles are the experimental results of Sohn *et al.* (1986).

0.6 eV. It is clear that the polarised SCF trial function quantitatively describes the Ramsauer minimum. Moreover, it is apparent that in the molecular case higher partial waves modify and partially obscure the dramatic RT minimum in the contribution from overall 2A_1 symmetry which is dominated by the s-wave.

Differential cross sections, in which partial waves for $l < 2$ are included in the Born approximation, are shown in Fig. 2. At 0.5 eV, near the location of the RT minimum, the sharp dip in the experimental cross section near 60° is not reproduced exactly by our complex Kohn calculations. However, at 3.0 eV the theoretical and experimental cross sections agree nearly exactly. It is substantially more difficult to reproduce differential cross sections in the RT energy range, because over that range the relative contributions of various partial waves are

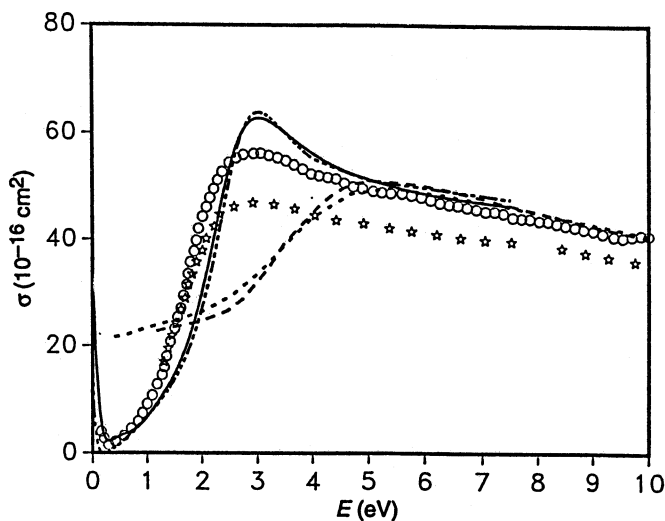


Fig. 3. Integrated cross sections for electron-silane elastic scattering. The dashed curve is the static-exchange result from Temkin and Lamkin (1961); dotted curve, the present static-exchange results with basis A; dot-dash curve, the polarised-SCF results with basis A; and solid curve, polarised-SCF results with basis B. Experimental results: stars, O. Sueoka (personal communication; see Winstead and McKoy 1990); circles, Wan *et al.* (1989).

changing rapidly, and the differential cross section changes radically with small energy changes, as we will demonstrate in another case below. Other calculations on CH_4 are discussed in Lengsfeld *et al.* (1991). These calculations were the first to indicate that the polarised SCF trial function is sufficient to provide a quantitative description of low-energy elastic collisions for a polyatomic target.

(3b) Low-energy Electron- SiH_4 Collisions

For our calculations on silane we employed a silicon basis of (11s, 6p)/[5s, 2p] contracted Gaussians augmented by (4s, 6p) diffuse functions. A (5s, 1p)/[3s, 1p] basis was used on the hydrogens. Two additional augmentations of diffuse Gaussians were used: (4d, 3f) on the silicon, to which we refer as basis A, and (7d) on silicon, which is basis B. The polarisabilities computed using basis sets A and B are $29.151a_0^3$ and $32.365a_0^3$, respectively, both of which compare favourably with the experimental value of $30.368a_0^3$.

In Fig. 3 we compare the calculated integral cross section with recent experiments. Several features of the calculation are immediately apparent. First of all, the static-exchange approximation fails totally to provide a description of the RT minimum and disagrees with experiment below 5 eV. Both basis A and basis B predict the RT minimum correctly, with the differences between the two calculations roughly indicating the uncertainty introduced by our finite basis expansion. Finally the d-wave shape resonance near 3 eV is correctly predicted, but appears slightly sharper than the experimental observation. There may be several reasons for that discrepancy, and we speculate that the fixed

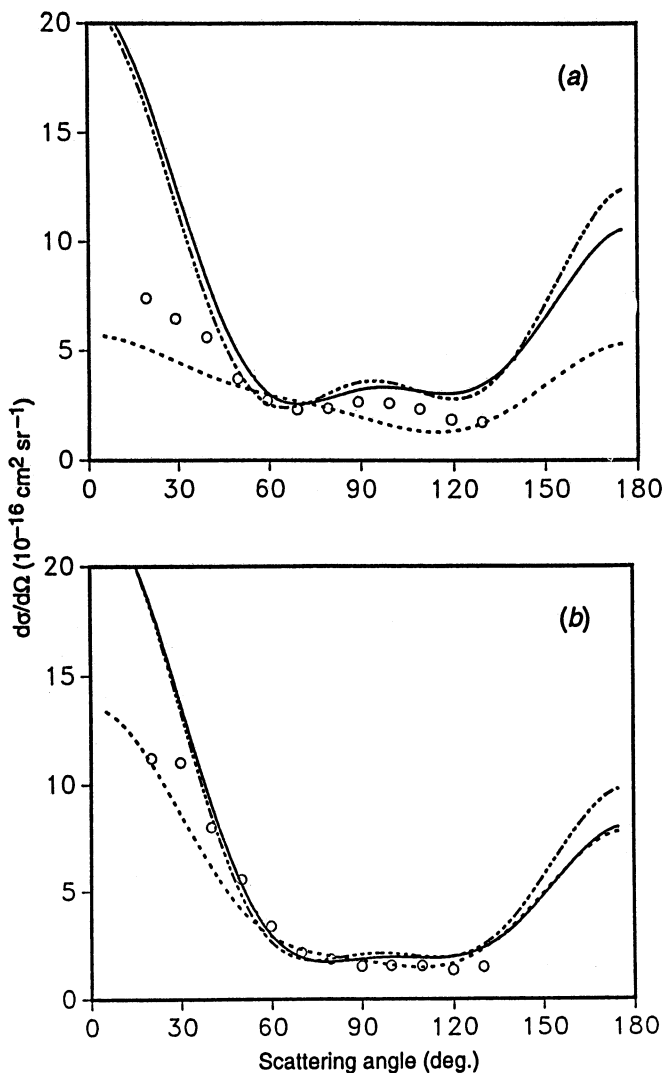


Fig. 4. Differential cross sections for electron-silane elastic scattering at (a) 3 eV and (b) 4 eV. The dash-dot curves are the polarised-SCF results with basis A; solid curves, the polarised-SCF results with basis B; and dotted curves, the static-exchange results with basis A. Circles are the experimental results of Tanaka *et al.* (1990).

nuclei approximation employed in these calculations may be a major cause, in addition to the contributions which a more complete treatment of correlation would include. Fig. 4a shows the differential cross section at 3 eV. While a clear d-wave character is seen in the calculated differential cross section, there is a significant discrepancy with experiment in the forward direction. On the other hand, at 4 eV, away from the resonance, there is much better agreement with experiment as shown in Fig. 4b.

Finally, we show the calculated differential cross sections in the RT region in Fig. 5. As the incident energy is scanned through the RT minimum the differential cross section changes radically. The s-wave contribution goes through

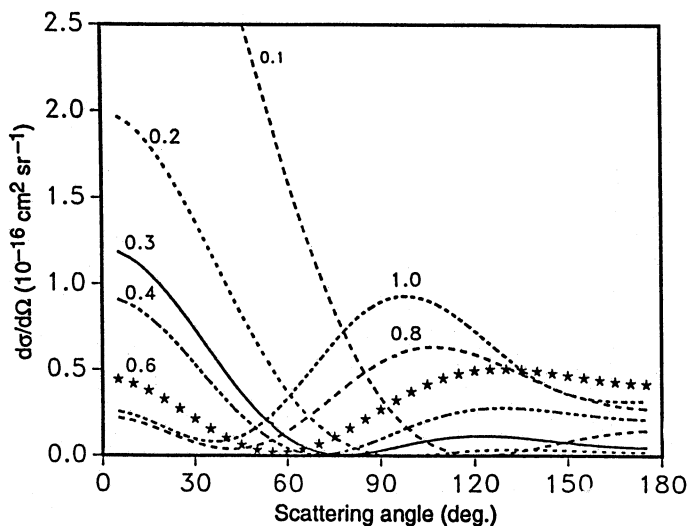


Fig. 5. Differential cross sections for electron-silane scattering below 1 eV using the complex polarised-SCF method and basis B. Each curve is labelled with the incident electron energy in eV.

a minimum and the interference with higher partial waves changes character rapidly. Our calculations suggest that such a rapid variation in differential cross section at low energies characterises RT minima in polyatomic molecules. The large size and asymmetry of these molecules results in significant contributions from higher partial waves in the RT region which can increase rapidly with increasing energy. Further calculations on low-energy electron-SiH₄ collisions are presented elsewhere (Sun *et al.* 1992a).

(3c) Low-energy Electron-C₂H₆ Collisions

The case of ethane is interesting because the low barrier to internal rotation (0.13 eV) allows a significant amount of hindered rotation at room temperature. One can therefore ask what is the effect on the electron scattering cross section of conformational changes in the molecule. For our calculations on ethane we employed a (10s, 6p, 1d)/[5s, 3p, 1d] contracted basis on the carbons and a (5s, 1p)/[2s, 1p] contracted basis on the hydrogens, together with (5s, 3p, 2d) functions at the centre of mass of the molecule. Two further augmentations with diffuse Gaussians were employed: basis A with (2p, 2d) diffuse functions at the centre of mass, and basis B with (3p, 3d, 3f) functions at the centre of mass.

In Fig. 6 we compare the integral cross sections computed at both the eclipsed and staggered geometries with available experiments. In the RT minimum region there is little difference between the results for the two conformers, but a significant difference is seen in the vicinity of the broad shape resonance near 7.5 eV. The shape resonance is predominantly f-wave in character. The staggered geometry produces a sharper, lower energy resonance, apparently because the presence of a centre of inversion in this conformer decouples even and odd values of the angular momentum quantum number l , and provides fewer couplings leading to the decay of the resonance. There are no experimental observations of the total

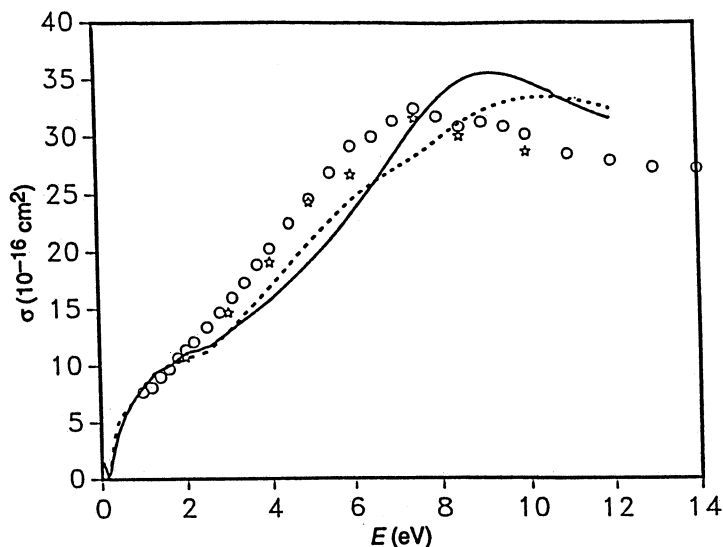


Fig. 6. Integrated cross sections for electron-ethane elastic scattering. The solid curve is the polarised-SCF result for staggered ethane with basis B; dotted curve, the polarised-SCF result for eclipsed ethane with basis B. The experimental results are: stars, Tanaka *et al.* (1988); circles, Sueoka and Mori (1986).

cross section below 2 eV available, and our calculations therefore predict a clear RT minimum will be seen near 0.18 eV, as suggested indirectly by momentum transfer measurements discussed below.

Differential cross sections are shown for 2 and 4 eV in Fig. 7. The strong d-wave character is apparent in these cross sections as well as the fact that there is only a small difference in the cross sections for eclipsed and staggered geometries at these energies. The similarity of the results for the two geometries is suggested by the small variation in polarisability with changing conformation. We find polarisabilities of $29.04a_0^3$ for the eclipsed and $29.20a_0^3$ for the staggered geometry, as compared with the experimental value of $30.17a_0^3$.

Finally, the momentum transfer cross section is shown in Fig. 8 and compared with values derived from two swarm experiments. The RT minimum is clearly seen in all the results. Above 0.3 eV the experimental determinations disagree with each other dramatically, and our results clearly suggest which is correct. Further results of our calculations on this system are presented elsewhere (Sun *et al.* 1992b).

4. Discussion

The simple polarised-SCF trial function described here apparently describes low-energy electron-polyatomic molecule collisions in near quantitative fashion, with a few discrepancies at shape resonances as we have noted. After our emphasis in Section 1 on the question of consistency in the treatment of N - and $(N+1)$ -electron correlation effects, one can ask how the polarised-SCF approach provides that consistency.

All of the Q -space configurations in the polarised-SCF trial function are formed by adding an electron to a configuration which is a single excitation from the

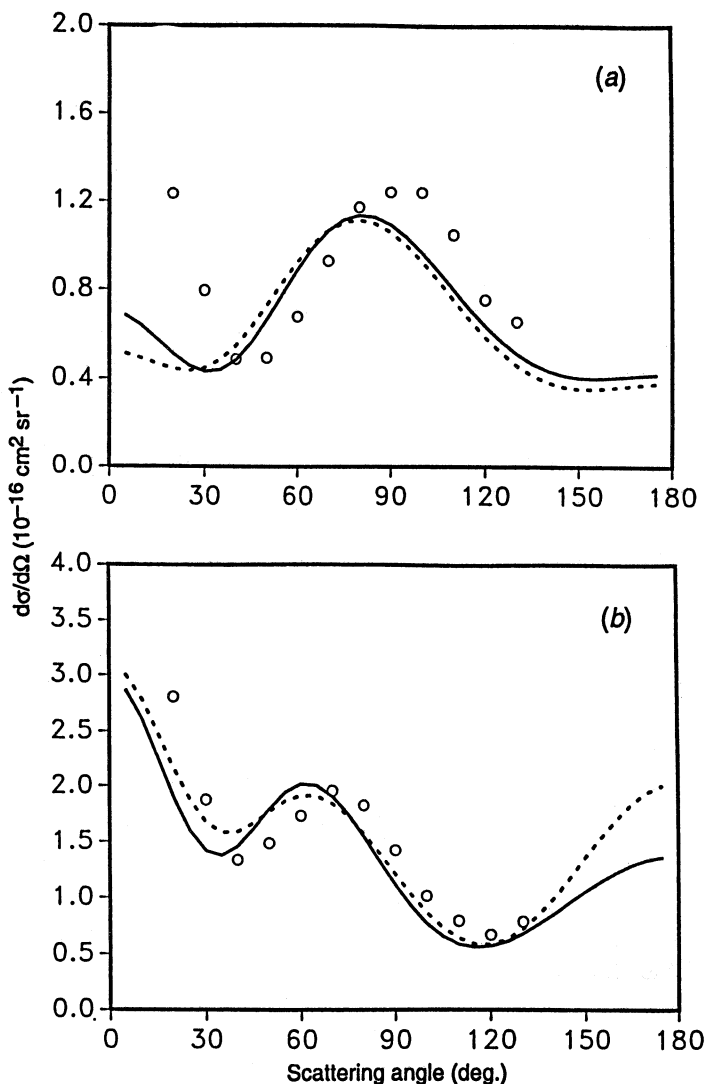


Fig. 7. Differential cross sections for electron-ethane scattering at (a) 2.0 eV and (b) 4.0 eV. Shown are the polarised-SCF results with basis B: solid curves for staggered ethane; dotted curves for eclipsed ethane. Circles are the experimental results from Tanaka *et al.* (1988).

Hartree-Fock target wavefunction. The P -space configurations are constructed by adding an electron to the target wavefunction. As the scattered electron recedes from the target the coupling between channels which remains is determined by a matrix element of the Hamiltonian between the Hartree-Fock ground state and a single excited configuration. That matrix element vanishes by Brillouin's theorem. This point is the underlying reason that the ground state wavefunction and energy are not modified implicitly by the inclusion of the Q -space correlating configurations in these calculations.

The case of correlated target wavefunctions is obviously more complicated, and we defer a discussion of that case to a later publication. The encouraging result of the studies reported here is that some common features, which are pure

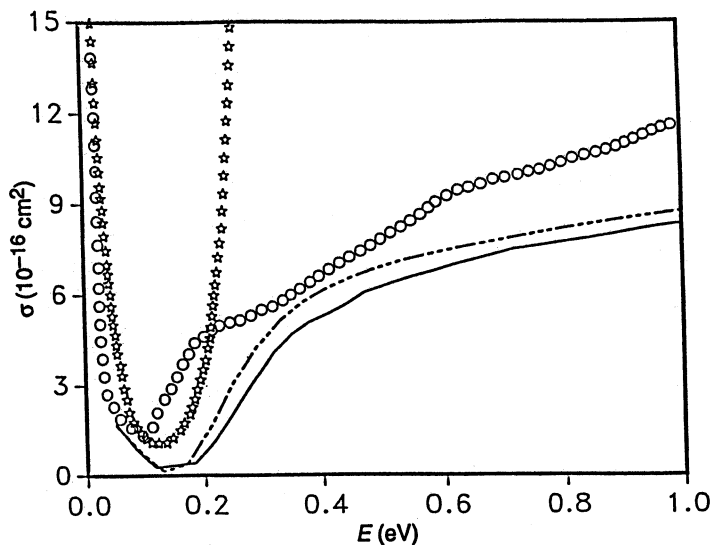


Fig. 8. Momentum transfer cross section given by the polarised-SCF results with basis B: solid curve for staggered ethane; dot-dash curve for eclipsed ethane. The experimental results are: circles, Duncan and Walker (1974); stars, McCorkle *et al.* (1978).

correlation effects, of electron-polyatomic molecule scattering are well described by this simple *ab initio* treatment of correlation.

Acknowledgments

This work was performed while the author was at Ohio State University and was supported by the National Science Foundation under Grant No. CHE-8922836 and by the Ohio Supercomputer Center.

References

- Callaway, J. (1957). *Phys. Rev.* **106**, 868.
 Callaway, J., LaBahn, R., Pu, R., and Duxler, W. (1968). *Phys. Rev.* **168**, 12.
 Duncan, C. W., and Walker, I. C. (1974). *J. Chem. Soc. Faraday II* **70**, 577.
 Lane, N. F. (1980). *Rev. Mod. Phys.* **52**, 29.
 Lengsfeld, B. H., III, Rescigno, T. N., and McCurdy, C. W. (1991). *Phys. Rev. A* **44**, 4296.
 Lima, M., Watari, K., and McKoy, V. (1989). *Phys. Rev. A* **39**, 4312.
 McCorkle, D. L., Christophorou, L. G., Maxey, D. V., and Carter, J. G. (1978). *J. Phys.* **B 11**, 3067.
 McCurdy, C. W., and Rescigno, T. N. (1989). *Phys. Rev. A* **39**, 4487.
 McCurdy, C. W., Rescigno, T. N., and Schneider, B. (1987). *Phys. Rev. A* **36**, 2061.
 Miller, W., and Jansen op de Haar, B. (1987). *J. Chem. Phys.* **86**, 6213.
 Parker, S. D., McCurdy, C. W., Rescigno, T. N., and Lengsfeld, B. H., III (1991). *Phys. Rev.* **A 43**, 3514.
 Rescigno, T. N., Lengsfeld, B. H., III, and McCurdy, C. W. (1990). *Phys. Rev. A* **41**, 2462.
 Rescigno, T. N., McCurdy, C. W., and Schneider, B. I. (1989). *Phys. Rev. Lett.* **63**, 248.
 Sohn, W., Kochem, K.-H., Scheuerlein, K.-M., Jung, K., and Ehrhardt, H. (1986). *J. Phys.* **B 19**, 3625.
 Sueoka, O., and Mori, S. (1986). *J. Phys. B* **19**, 4035.
 Sun, W., McCurdy, C. W., and Lengsfeld, B. H., III (1992a). *Phys. Rev. A* **45**, 6323.

- Sun, W., McCurdy, C. W., and Lengsfeld, B. H., III (1992*b*). *Ab initio* study of low-energy electron-ethane scattering. *Phys. Rev. A* (in press).
- Takasuka, K., and McKoy, V. (1981). *Phys. Rev. A* **24**, 2473.
- Takasuka, K., and McKoy, V. (1984). *Phys. Rev. A* **30**, 1734.
- Tanaka, H., Boesten, L., Matsunaga, D., and Kudo, T. (1988). *J. Phys. B* **21**, 1255.
- Tanaka, H., Boesten, L., Sato, H., Kimura, M., Dillon, M. A., and Spence, D. (1990). *J. Phys. B* **23**, 577.
- Taylor, J. R. (1972). 'Scattering Theory', p. 382 (Wiley: New York).
- Temkin, A. (1957). *Phys. Rev.* **107**, 1004.
- Temkin, A. (1959). *Phys. Rev.* **116**, 385.
- Temkin, A., and Lamkin, J. (1961). *Phys. Rev.* **121**, 788.
- Wan, H.-X., Moore, T. H., and Tossel, J. A. (1989). *J. Chem. Phys.* **91**, 7340.
- Winstead, C., and McKoy, V. (1990). *Phys. Rev. A* **42**, 5357.

Manuscript received 11 March, accepted 26 May 1992